

Kondo Lattice Behavior Observed in the CeCu₉In₂ Compound

R. Kurleto^a, A. Szytuła^a, J. Goraus^b, S. Baran^a, Yu. Tyvanchuk^c, Ya. M. Kalychak^c, P. Starowicz^a

^aMarian Smoluchowski Institute of Physics, Jagiellonian University, Łojasiewicza 11, 30-348 Kraków, Poland

^bInstitute of Physics, University of Silesia, 75 Pułku Piechoty 1a, 41-500 Chorzów, Poland

^cDepartment of Analytical Chemistry, Ivan Franko National University of Lviv, Kyryla and Mephodiya 6, 79005 Lviv, Ukraine

Abstract

We report systematic studies of CeCu₉In₂, which appears to be a new Kondo lattice system. Electrical resistivity exhibits a logarithmic law characteristic of Kondo systems with a broad maximum at $T_{coh} \approx 45$ K and it obeys the Fermi liquid theory at low temperature. Specific heat of CeCu₉In₂ is well described by the Einstein and Debye models with electronic part at high temperature. Fitting of the Schottky formula to low temperature 4f contribution to specific heat yielded crystal field splitting of 50.2 K between a doublet and quasi-quartet. The Schotte-Schotte model estimates roughly Kondo temperature as $T_K \approx 5$ K, but does not reproduce well the data due to a sharp peak at 1.6 K. This structure should be attributed to a phase transition, a nature of which is possibly antiferromagnetic. Specific heat is characterized with increased Sommerfeld coefficient estimated as $\gamma \approx 132$ mJ/(mole·K²). Spectra of the valence band, which have been collected with ultraviolet photoelectron spectroscopy (UPS), show a peak at binding energy ≈ 250 meV, which originates from the Ce 4f electrons and is related to the 4f¹_{7/2} final state. Extracted 4f contribution to the spectral function exhibits also the enhancement of intensity in the vicinity of the Fermi level. Satellite structure of the Ce 3d levels spectra measured by X-ray photoelectron spectroscopy (XPS) has been analyzed within the framework of the Gunnarsson-Schönhammer theory. Theoretical calculations based on density functional theory (FPLO method with LDA+U approach) delivered densities of states, band structures and Fermi surfaces for CeCu₉In₂ and LaCu₉In₂. The results indicate that Fermi surface nesting takes place in CeCu₉In₂.

Keywords: rare earth alloys and compounds, Kondo effect, heat capacity, electrical transport, photoelectron spectroscopies, electronic band structure

1. Introduction

Presence of unpaired 4f electron in cerium atom leads to many unusual physical phenomena in cerium intermetallic compounds. Often, experimental evidence points to a dichotomous character of 4f electrons, which are neither fully localized nor fully itinerant. This plays an important role in physics of such systems. These electrons form a relatively narrow band, which hybridizes with carriers from a conduction band. This coupling can lead to quenching of magnetic moments of f electrons and to formation of singlets in a ground state. Other complex states, such as a Kondo lattice or a mixed valency are also possible. The aforementioned dynamic singlet state in a Kondo regime is manifested by a pronounced anomaly in an electrical resistivity and by the so called Kondo peak in a spectral function. While the presence of the latter feature in a single impurity regime (Kondo regime) is well established, analogous spectral shape in the case of a Kondo lattice may be an interesting subject of research.

Crystal chemistry of ternary indides with rare-earth and transition metal elements was the subject of previous studies due to intriguing physical properties [1, 2, 3].

The structural phase diagram of the Ce–Cu–In system was constructed previously and extensively discussed [1, 4, 5]. CeCu₉In₂ compound crystallizes in the YNi₉In₂-type tetragonal structure (P4/mbm space group), with lattice constants: $a=8.5403(4)$ Å and $c=5.0204(5)$ Å. LaCu₉In₂ is isostructural to CeCu₉In₂. Its crystal structure, specific heat and magnetic susceptibility were reported before [6]. Lattice constants of LaCu₉In₂ slightly differ from those obtained for the cerium counterpart ($a=8.6351(4)$ Å, $c=5.1488(3)$ Å). Both intermetallic compounds are characterized by narrow homogeneity ranges with substitution of Cu by In [1]. Specific heat of LaCu₉In₂ is well modeled by the sum of phononic and electronic contributions (details of the fitting procedure are available elsewhere [6]). The magnetic susceptibility of LaCu₉In₂, measured at 0.1 T and 1 T, is almost temperature independent. This fact was interpreted as a symptom of a Pauli paramagnetism [6]. It should be mentioned that replacement of a transition metal may have a significant effect; recently, a mixed valence state has been proposed for the isostructural CeNi₉In₂ compound [3, 7, 8, 9].

Magnetic properties of CeCu₉In₂ were studied before [6]. Measured magnetic susceptibility follows the Curie-Weiss law in a broad temperature range (100-350 K). The estimated Curie-Weiss temperature is equal to -39 K, while inferred value of effective magnetic moment is slightly enhanced to $\mu=2.88 \mu_B$, which can be compared to $\mu=2.54 \mu_B$,

Email addresses: rafal.kurleto@uj.edu.pl (R. Kurleto), pawel.starowicz@uj.edu.pl (P. Starowicz)

what is a theoretical value for free Ce^{3+} [6]. This value suggests that valency of cerium is close to 3.

In this article we describe physical properties of the $CeCu_9In_2$ compound. Namely, we provide electrical resistivity, specific heat, as well as photoelectron spectra of the valence band and Ce 3d levels. In order to reveal the role of the 4f electrons we have also performed measurements on isostructural $LaCu_9In_2$. The obtained spectra are confronted with the results of theoretical calculations. We have analyzed our data in terms of the Kondo lattice with the Fermi liquid ground state. Our results testify significant coupling between the 4f electrons and carriers from the conduction band in $CeCu_9In_2$. This compound is a new system in which a realization of a Kondo lattice takes place.

2. Materials and methods

Fabrication and characterization of polycrystalline samples of $CeCu_9In_2$ and $LaCu_9In_2$ (the latter with exact stoichiometry: $LaCu_{8.25}In_{2.75}$) were described elsewhere [6]. Electrical resistivity has been measured with application of four-terminal alternating current technique in Physical Property Measurement System (PPMS, Quantum Design) in temperature range 2–300 K. Specific heat has also been measured in PPMS, with application of a relaxation method (two-tau model), in similar temperature range. Additional measurement of specific heat in temperature range 0.4–10 K has been performed with application of 3He refrigerator.

Photoelectron spectroscopy has been conducted with an in-house experimental setup, equipped with VG Scienta R4000 photoelectron energy analyzer. X-ray photoelectron spectroscopy (XPS) has been performed with application of Mg K_{α} ($h\nu=1253.6$ eV) and Al K_{α} ($h\nu=1486.6$ eV) radiation (without a monochromator) at temperature: 12.5 K, 100 K or 292 K. He I ($h\nu=21.2$ eV) and He II ($h\nu=40.8$ eV) spectral lines from helium lamp have been used in the ultraviolet photoelectron spectroscopy (UPS) studies. Spectra have been collected at the same temperatures as the ones from XPS. Both XPS and UPS measurements do not reveal any significant change in the function of temperature, so further in the article we present only spectra collected at the lowest possible temperature (12.5 K). Base pressure during measurements was equal to $5 \cdot 10^{-11}$ mbar. Before measurements, surface of the samples was polished under ultra high vacuum conditions (base pressure $2 \cdot 10^{-10}$ mbar) with application of a diamond file. Calibration was provided by a measurement of binding energy of the Au 4f states on polycrystalline gold layer and by measurement of Fermi edge of polycrystalline Cu for XPS and UPS measurements, respectively.

Full potential local orbital (FPLO) code [10] in scalar relativistic version has been used in order to obtain partial densities of states (DOS) of $CeCu_9In_2$ and $LaCu_9In_2$. Additional correlations have been involved in around mean field scheme with application of local spin density approximation (LSDA+U) [11]. Perdew-Wang exchange-correlation potential [12, 13] has been assumed in calculations. In case of the compound with cerium, DOS have been obtained for Coulomb repulsion on the f shell equal to 0 eV, 2 eV (not

shown in this paper) and 6 eV. The band dispersion along important crystallographic directions in k-space as well as Fermi surface (FS) of both studied compounds have been calculated with application of Elk software [14]. The results from FPLO and Elk are consistent. All theoretical calculations have been performed assuming non-magnetic state of $CeCu_9In_2$, what corresponds to a paramagnetic state for which the photoemission spectroscopy has been realized.

3. Results and Discussion

3.1. Electrical resistivity

Electrical resistivity of the $CeCu_9In_2$ compound, measured as a function of temperature, exhibits a pronounced anomaly (Fig. 1 a). There is a broad maximum clearly visible at temperature equal to 45 K. At low temperature ($T < 13$ K) resistivity is well described by the quadratic function:

$$\rho = \rho_0 + AT^2. \quad (1)$$

Obtained residual resistivity ρ_0 is equal to $70.10(1) \mu\Omega \cdot \text{cm}$, while A coefficient reaches $10.2(2) \cdot 10^{-3} \mu\Omega \cdot \text{cm}/\text{K}^2$. This behavior implies that a coherent Fermi liquid is developed below 13 K in the studied system. Temperature variation of electrical resistivity for $CeCu_9In_2$ is typical of Kondo lattice systems and the broad maximum yields a coherence temperature of $T_{coh} \approx 45$ K. It should be mentioned that the equation (1) with an additional T^5 term representing phonon scattering was also fitted to experimental data but the quality of the fit did not improve considerably.

We have also measured electrical resistivity of the $LaCu_9In_2$ compound (Fig. 1 b), which has got the same crystal structure as $CeCu_9In_2$. Temperature dependence of electrical resistivity for $LaCu_9In_2$ does not exhibit any pronounced anomaly. Its shape is typical of a simple metal, besides some small concavity, which is most probably due to s-d scattering. We have found that experimental data are described well by the Grneisen–Bloch–Mott model [15, 16]. The fitted function has got the following form:

$$\rho = \rho_0 + c \frac{T}{\theta} \int_0^{\frac{\theta}{T}} \frac{x^5 dx}{(e^x - 1)(1 - e^{-x})} - KT^3, \quad (2)$$

where: ρ_0 is a residual resistivity, θ denotes the Debye temperature, c is a parameter related to the electron-phonon coupling, while K is the Mott coefficient, which describes the strength of interband s-d scattering. The obtained values of the parameters are as follows: $\rho_0 = 45.33(2) \mu\Omega \cdot \text{cm}$, $c = 82.2(8) \mu\Omega \cdot \text{cm}$, $\theta = 189(2)$ K, $K = 1.9 \cdot 10^{-7} \mu\Omega \cdot \text{K}^{-3} \cdot \text{cm}$.

The measured electrical resistivities of both compounds have been used in order to estimate magnetic contribution of Ce 4f states (ρ_m) to electrical transport in $CeCu_9In_2$. It was obtained by a subtraction of $LaCu_9In_2$ data from those measured for Ce counterpart (Fig. 1 c). The obtained shape is consistent with previous studies of Kondo lattice systems [17]. Beyond the aforementioned broad maximum we have found that logarithmic dependency is

obeyed between 58 K and 165 K. The fit of the formula proposed by J. Kondo:

$$\rho_m = b_1 + b_2 \ln T, \quad (3)$$

yielded $b_1=91.1(3) \mu\Omega\cdot\text{cm}$ and $b_2=-15.54(5) \mu\Omega\cdot\text{cm}$.

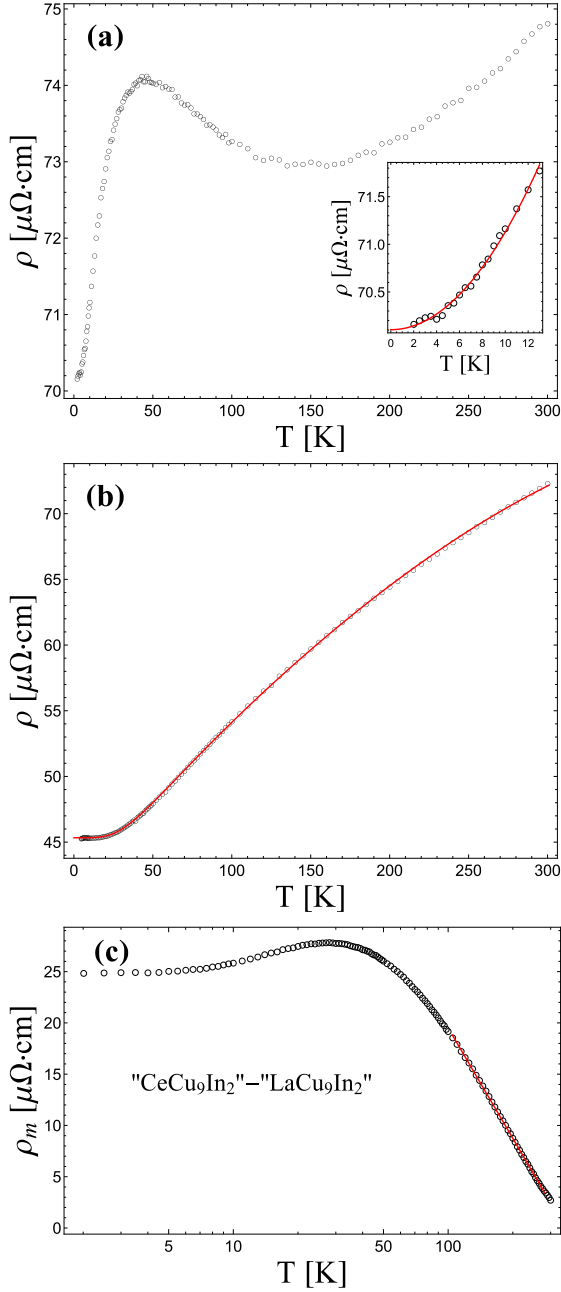


Figure 1: (Color on-line) (a) Temperature variation of the electrical resistivity (black circles) of CeCu_9In_2 . The red line represents fitted model. Inset: the electrical resistivity at low temperature (2-13 K) with fitted model characteristic of the Fermi liquid (1). (b) Temperature variation of the electrical resistivity (black circles) of LaCu_9In_2 . The red line represents fitted Grneisen-Bloch-Mott formula (2). (c) Extracted Ce 4f contribution to the electrical resistivity (black circles) of CeCu_9In_2 with fitted Kondo law (3) in temperature range 58-165 K.

3.2. Specific heat

The investigated compounds were also subjected to studies of specific heat (Fig. 2). High temperature part of specific heat (Fig. 2 a) for the CeCu_9In_2 compound is described

well by the sum of lattice contributions (Debye and Einstein models) and electronic part. Namely, we have used the formula:

$$c = \gamma'T + 9kNR \left(\frac{T}{\theta}\right)^3 \int_0^{\frac{\theta}{T}} \frac{x^4 dx}{(e^x - 1)^2} + 3(1-k)R \left(\frac{\theta_E}{T}\right)^2 \frac{e^{\frac{\theta_E}{T}}}{\left(e^{\frac{\theta_E}{T}} - 1\right)^2}, \quad (4)$$

where: γ' represents a linear term, k is relative weight of Debye and Einstein modes, θ_E is the Einstein temperature, $N=12$ is the number of atoms in the unit cell, R is the universal gas constant. Obtained values are as follows: $\theta=246(8)$ K, $\gamma'=121(8)$ mJ/(mole $\cdot\text{K}^2$), $\theta_E=176(129)$ K, $k=0.64(3)$.

At low temperature, we have plotted c/T versus T^2 (see inset to Fig. 2 a). We have found a linear dependency in the temperature range between 10 K and 20 K. The linear fit yielded $\gamma = 132(4)$ mJ/(mol $\cdot\text{K}^2$), as well as the Debye temperature equal to 107.8 K, which is much lower than the value obtained for high temperature fit to the equation (4). The value of γ is close to γ' resulting from fitting more complex formula (4). Although, the temperatures taken for the linear fit were relatively high for the obtained value of θ [18] the fitted γ is some estimation of Sommerfeld coefficient. Its high value indicates that charge carriers in CeCu_9In_2 have got high effective masses. This fact also implies high value of the density of states at the Fermi level.

Significant anomalies are found at low temperature specific heat. Magnetic contribution related to 4f electrons has been estimated (Fig. 2 b) by a subtraction of the specific heat measured for the isostructural LaCu_9In_2 compound. One can see three peak-like structures at low temperature. The first one is sharp and located at about 1.6 K (cf. Fig. 2 b). The contribution from the Kondo effect is expected at such temperature. It can be described in terms of the Schotte-Schotte model [19]. It was argued before that such model applies even in a Kondo lattice regime: $\text{Ce}_{1-x}\text{La}_x\text{Ni}_2\text{Ge}_2$ [20]. The second, broad peak is located roughly at 22 K. According to our knowledge, it is related to crystal field effects, described by the modified Schottky formula [21]. The third, additional λ -type peak at about 7 K is related to the presence of small amount of cerium sesquioxide (Ce_2O_3) [22]. It is known, that cerium ion, confined in symmetry different than cubic, should have crystal field configuration, which consists of three doublets. In CeCu_9In_2 , Ce atoms occupy $2a$ site of $P4/m3m$ space group, which is characterized by tetragonal symmetry (site symmetry: $4/m..$). However, our data can be described properly by the Schottky formula with a doublet-quartet configuration, which should be observed in case of cubic symmetry. Our attempts of fitting the model with three doublets have led to the results with unreliable coefficients. This discrepancy may be explained by the fact that splitting energy for two doublets is too small to be resolved and therefore a quasi-quartet results from fitting. Similarly, such a quasi-quartet state was observed in case of hexagonal CeCu_4Al [23]. Finally, the fitted model has got a form:

$$c_{4f} = c_{cf} + c_K + \gamma^*T, \quad (5)$$

where c_{cf} stands for contribution related to crystal field:

$$c_{cf} = \frac{8e^{-\frac{\Delta}{T}} R \Delta^2}{(4 + 2e^{-\frac{\Delta}{T}}) 2T^2} \quad (6)$$

(R -universal gas constant, Δ -quartet-doublet splitting), while c_K denotes a contribution related to a Kondo scattering given by the Schotte-Schotte model:

$$c_K = R \frac{T_K}{T\pi} \left[1 - \frac{T_K}{2T\pi} \psi' \left(\frac{1}{2} + \frac{T_K}{2T\pi} \right) \right] \quad (7)$$

(R -universal gas constant, T_K -Kondo temperature, ψ' first derivative of digamma function).

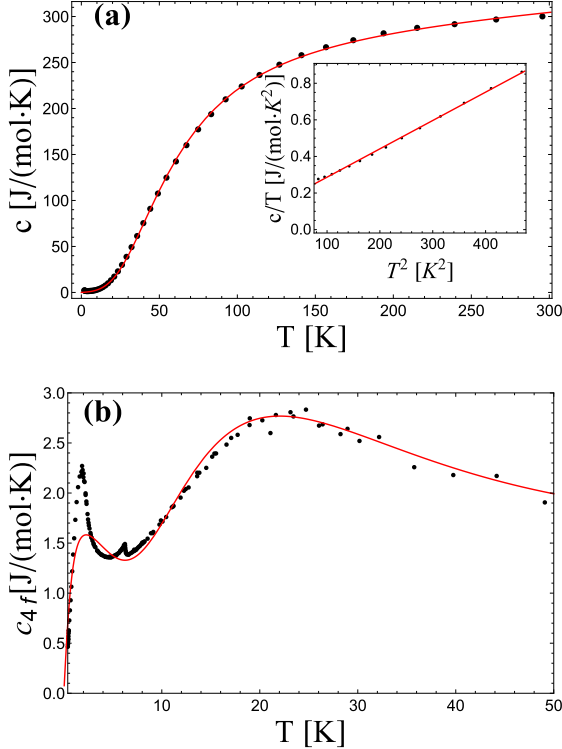


Figure 2: (Color on-line) (a) Specific heat of CeCu_9In_2 (black points). Red line is a result of the fitted model (4). Inset: c/T vs T^2 dependency with the fitted line. (b) Magnetic contribution of 4f electrons to the specific heat of CeCu_9In_2 (black points). The red line corresponds to the fit of the sum of contributions from the Schotte-Schotte model and the Schottky model (5).

γ^* coefficient obtained from the fit of equation (5) to the data equals $13.4(1.9)$ mJ/(mole·K²). Fitting procedure yielded Kondo temperature (T_K) equal to $4.6(3)$ K and a doublet-quartet splitting Δ equal to $50.2(1.1)$ K. The effect of correlation between charge carriers is included in both Schotte-Schotte and linear contribution to specific heat. Hence, the value of γ^* is not a good measure of the mass enhancement. Indeed for $T \ll T_K$ the Schotte-Schotte model can be linearized and its contribution to a linear term is not included in γ^* . Therefore the obtained small value of γ^* underestimates the renormalization factor for the electron mass.

One can see that the agreement between the fitted model (eq. 5, cf. Fig. 2 b) and experimental data is not perfect, especially below 6 K. In particular, a phase transition, which has been not considered so far, can be reflected in a peak

at 1.6 K. In fact, there are premises, which point to the appearance of the transition to antiferromagnetic state in the CeCu_9In_2 compound at low temperature. Namely, these are a negative value of the paramagnetic Curie-Weiss temperature and a significant deviation of magnetic susceptibility from the Curie-Weiss law at low temperature [6]. Magnetic entropy was calculated using estimated Ce 4f contribution to the specific heat. At the temperature of the peak at $T = 1.6$ K it reaches about 45% of a theoretical value $R \ln 2$, corresponding to a doublet ground state. The reduced value of the magnetic entropy points to significance of the Kondo interaction in the studied compound.

3.3. Valence band photoelectron spectra

Many interesting properties of systems with interacting electrons are reflected in the spectral function. In order to study impact of the Kondo effect on the spectral function we have measured UPS spectra of the valence band of the studied compound. One of the fingerprints of the Kondo effect is the Kondo peak. In heavy fermion compounds maximum of the Kondo peak should lie at δ energy above Fermi level according to the Friedel formula [24]:

$$\delta = k_B T_K \sin(\pi n_f), \quad (8)$$

where: n_f is a mean occupation of 4f level, T_K is a Kondo temperature. Usually in photoemission experiments, one can observe only the tail of the Kondo peak, i.e. the peak is sharply cutted by the Fermi edge. The Kondo peak itself is assigned to the $4f_{5/2}^1$ final state in the UPS spectra of the valence band. For the parameters corresponding to our study; $n_f = 0.96$, $T_K = 4.6$ K, according to (8) δ is of order of 0.05 meV, which should locate the Kondo peak very close to the Fermi energy.

UPS spectra of the valence band of CeCu_9In_2 in vicinity of the Fermi level, measured with He-II and He-I radiation are shown in the Fig. 3 a. In both, He-II and He-I spectra, the tail of the Kondo peak at the Fermi level is not visible. However, in both spectra, one can see some small peak superimposed on the linear slope at binding energy equal to -0.28 eV. This structure can be assigned to $4f_{7/2}^1$ final state in the photoemission process. We have estimated 4f contribution to the spectral function of CeCu_9In_2 by subtracting He-I from the He-II spectrum [25, 26]. Such 4f spectral weight yields slightly increased intensities near the Fermi energy (E_F) and at -0.28 eV, which are attributed to the $4f_{5/2}^1$ and $4f_{7/2}^1$ final states, respectively. The intensity near E_F may originate from a Kondo peak, which is hardly visible in this case.

UPS spectra of the valence band of isostructural LaCu_9In_2 have also been measured. One can see that He-II spectrum of LaCu_9In_2 , in contrary to that for CeCu_9In_2 , is completely featureless in the vicinity of the Fermi level. 4f contribution to the spectral function of CeCu_9In_2 has also been estimated by subtracting He-II spectrum for LaCu_9In_2 from He-II spectra for CeCu_9In_2 (Fig. 3 b). The obtained result is similar to the difference between He-II and He-I spectra for CeCu_9In_2 . However, in this case the increased intensity near E_F is not well visible. A sharp Kondo peak is not

found. Except for the absence of a sharp, coherent peak at the Fermi level, our spectral function resembles that usually observed for Kondo lattice systems [27].

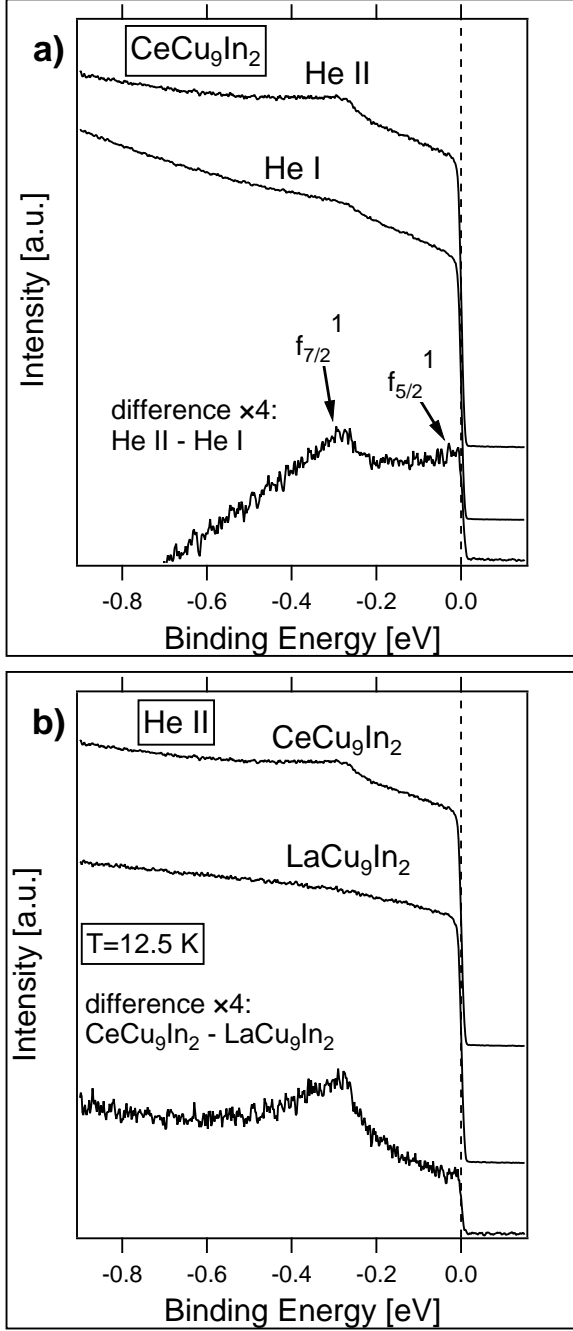


Figure 3: (a) UPS spectra of valence band of CeCu₉In₂ obtained with He-II (40.8 eV) and He-I (21.2 eV) radiation at the temperature equal to 12.5 K. 4f contribution to the spectral function, estimated by subtraction of He-I spectrum from He-II spectrum, is presented. Peaks corresponding to the $f_{7/2}^1$ and $f_{5/2}^1$ final states are marked by arrows. (b) Comparison between CeCu₉In₂ and LaCu₉In₂ He-II spectra of valence band. The calculated difference is also an estimation of Ce 4f electrons contribution.

There can be several reasons which render difficulty in observation of a Kondo peak. For instance, the applied experimental resolution of 13 meV might be not sufficient to record such a sharp feature. Moreover, polycrystalline samples obtained by arc-melting may exhibit certain disorder in particular at the surface, which can suppress spectral intensity

at E_F . It is also worth to compare spectra presented here for CeCu₉In₂, with those reported previously for CeNi₉In₂ [9]. In case of the compound with Ni, the Ni 3d states are located almost at the Fermi level and interact strongly with f states resulting in the mixed valence state. In case of compounds with Cu, the Cu 3d states are rather distant from the Fermi level, making interaction with 4f states weaker and resulting in the Kondo lattice state.

We would like to refer to the results reported previously for CeCu₆. This system is an archetypal heavy fermion compound, which displays the Kondo lattice behavior without magnetic ordering down to 5 mK [28, 29]. Specific heat as well as magnetic susceptibility of this compound are enhanced at low temperatures. Its electrical resistivity shows a maximum at low temperature, similarly to our results obtained for CeCu₉In₂. Although fingerprints of Kondo lattice state are clearly visible in electronic transport, the influence of the Kondo effect on the UPS spectra of the valence band of CeCu₆ is barely seen in certain reports [30, 31]. Namely, in the He-II spectra, there is no any sharp peak at the Fermi level. However, there is a peak visible at the binding energy equal to -0.25 eV, which was attributed to $f_{7/2}^1$ final state. According to the results of inelastic neutron scattering experiment [32], the CeCu₆ compound has got $T_K = 5$ K. It is commonly believed, that the value of T_K is related to the shape of the UPS spectrum. Namely, the ratio of intensities $I(f_{5/2}^1)/I(f_{7/2}^1)$ is a monotonic, increasing function of T_K . So, when the T_K is small, the intensity of the Kondo peak with respect to its spin-orbit partner is very low. Some studies of heavy fermion systems with low value of T_K , state that in order to observe the Kondo peak in the UPS spectra, one should measure with resolution less than $k_B T_K$ [33]. This statement was confirmed by recent measurements on CeCu₆, in which the authors reported the Kondo peak in the spectra [34, 35]. Possibly, the situation in case of CeCu₉In₂ is the same as for CeCu₆. Analysis of the specific heat of CeCu₉In₂ yields very low value of T_K (about 5 K), and the He-II spectrum resembles the early spectra of CeCu₆.

3.4. XPS of Ce 3d levels

Strong Coulomb interaction between 4f electrons and photoholes created in core levels during photoemission process leads to characteristic satellite structure of the XPS spectrum of Ce 3d levels. Each spin orbit partner in 3d doublet splits into three satellites corresponding to different numbers of electrons on the f shell in the final state of photoemission process. Fitting procedure applied together with the so called Gunnarsson-Schönhammer theory [36, 37] allows to estimate parameters such as a mean occupation of 4f shell, as well as the strength of the coupling between conduction band and 4f level.

XPS spectrum of Ce 3d levels of CeCu₉In₂ is shown in the Fig. 4. Peak deconvolution and numerical analysis can be based on the Doniach-Šunjić theory [38]. The background has been simulated with application of the Shirley method [39]. Peaks corresponding to the Ce 3d_{5/2} and Ce 3d_{3/2} levels are clearly visible. They are separated by spin-orbit splitting equal to 18.5 eV. Each component of

the doublet is further splitted due to the hybridization effects. Namely, each component of the doublet consists of three satellite lines: f^0 , f^1 and f^2 . The $3d^94f^0$ component is an evidence of the intermediate valence state of cerium ions, while the $3d^94f^2$ component gives information about the hybridization between 4f states and conduction electron states. Locations as well as intensities of particular peaks are collated in Table 1.

Table 1: Binding energies (E_B) and relative intensities (I) of satellite lines in XPS spectra of Ce 3d levels. We present results obtained for the $3d_{5/2}$ component. Spin-orbit splitting is equal to 18.5 eV.

$3d_{5/2}$	f^0	f^1	f^2
E_B [eV]	897.45	884.50	881.97
I [a.u.]	0.06	1	0.37

Satellites corresponding to the f^0 and f^2 final states are not fully resolved — they are visible as shoulders of the intense f^1 line. According to the theoretical model [36, 37], the intensity ratio $r_1 = I(f^0)/[I(f^0) + I(f^1) + I(f^2)]$ yields information about the occupation of Ce 4f shell $n_f = 1 - r_1$. We have obtained the value $n_f=0.96$. The hybridization energy can be estimated from the ratio $r_2 = I(f^2)/[I(f^1) + I(f^2)]$. The value of r_2 equal to 0.27 corresponds to the hybridization energy equal to 139 meV.

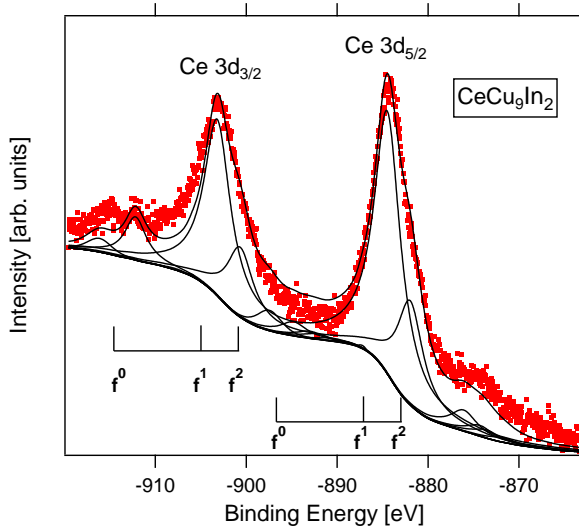


Figure 4: (Color on-line) XPS spectra of the Ce 3d levels in CeCu_9In_2 obtained with Mg K_α radiation at the temperature equal to 12.5 K. Experimental data are denoted by red dots, while solid black lines correspond to the fitted model.

3.5. Theoretical calculations

Theoretical calculations have been performed in order to get insight into the electronic structure of the studied compounds and to have a comparison with our experimental results. Total and partial densities of states, calculated for LaCu_9In_2 and CeCu_9In_2 with application of FPLO code, are shown in Fig. 5. In case of CeCu_9In_2 densities of states have been calculated within two computational schemes: without interaction between f electrons ($U=0$ eV, Fig. 5 b) and with Coulomb repulsion on 4f shell ($U=2$ eV not shown, $U=6$ eV, Fig. 5 c).

Density of states in the valence band of LaCu_9In_2 is dominated by the Cu 3d states (Fig. 5 a). There is some humped structure build up from those states, mostly located between -5 eV and -1 eV. In the vicinity of the Fermi level, La 5d, In 5s and 5p states contribute to the total density of states. La 5d states extend mostly above the Fermi level, while In 5s and 5p are rather smeared over the whole valence band.

In case of CeCu_9In_2 we have performed calculations for different values of Coulomb repulsion (U) between electrons on 4f shell. Densities of states calculated for $U=0$ eV, are symmetric and one can notice that for Cu and In, they are roughly the same as in case of the compound with La. In partial density originating from Ce, contribution from 4f orbital character is very significant. Namely, there is a sharp peak, located at about 0.3 eV above the Fermi level. For $U=6$ eV the density of states is considerably modified. While the partial densities of states related to Cu and In remain roughly unchanged, there is an important change in case of partial Ce 4f DOS. This quantity is not symmetric with respect to the spin degrees of freedom. One can see that, for arbitrary chosen, "up" component of the spin, 4f DOS has two dominating structures. The first one is the peak at binding energy equal to -4 eV, the second one is the peaked structure, which is located above the Fermi level. The maximum of the latter structure is at about 2 eV. 4f DOS related to "down" component of the spin has got only one, hump-like structure. This feature lies above the Fermi level, with the maximum at about 1.7 eV. The asymmetry of the 4f, as well as total DOS, can lead to a presence of some spontaneous magnetic moment in the ground state of the CeCu_9In_2 compound. We have also performed calculation for $U=2$ eV, however they are not qualitatively different from those for $U=0$ eV.

The band dispersion along some high symmetry lines inside first Brillouin zone (BZ) (Fig. 6), as well as FS (Fig. 7), have been calculated for CeCu_9In_2 and LaCu_9In_2 . For both compounds, calculations have been done under assumption of non-magnetic ground state. One can notice, that far from the Fermi level, the bands have got similar dependency on the \mathbf{k} -vector. In the band structure of CeCu_9In_2 , one can observe some structures which are absent in case of LaCu_9In_2 . These are six flat bands visible above the Fermi level. They extend from about 0.2 eV to about 0.4 eV above the Fermi level. These states are mostly related to 4f orbital character. So, according to the theoretical calculations, 4f states in CeCu_9In_2 are not localized and are characterized by large effective masses. For both compounds one can observe some broad hole pocket around the center of the Γ -Z line. Beyond this fact, the band structure in the vicinity of the Fermi level is quite different for studied compounds and this fact is reflected in the calculated FS. FS (Fig. 7) of both compounds is strongly anisotropic. In case of LaCu_9In_2 4 bands contribute to FS, while in case of CeCu_9In_2 there are only 3 bands which cross the Fermi level. For the compound with La, one can see a feature in the center of BZ (around the Γ point) flattened in the direction perpendicular to \mathbf{c}^* . This structure is surrounded, symmetrically in the \mathbf{c}^* direction, by highly corrugated leaf-like structures. In case of

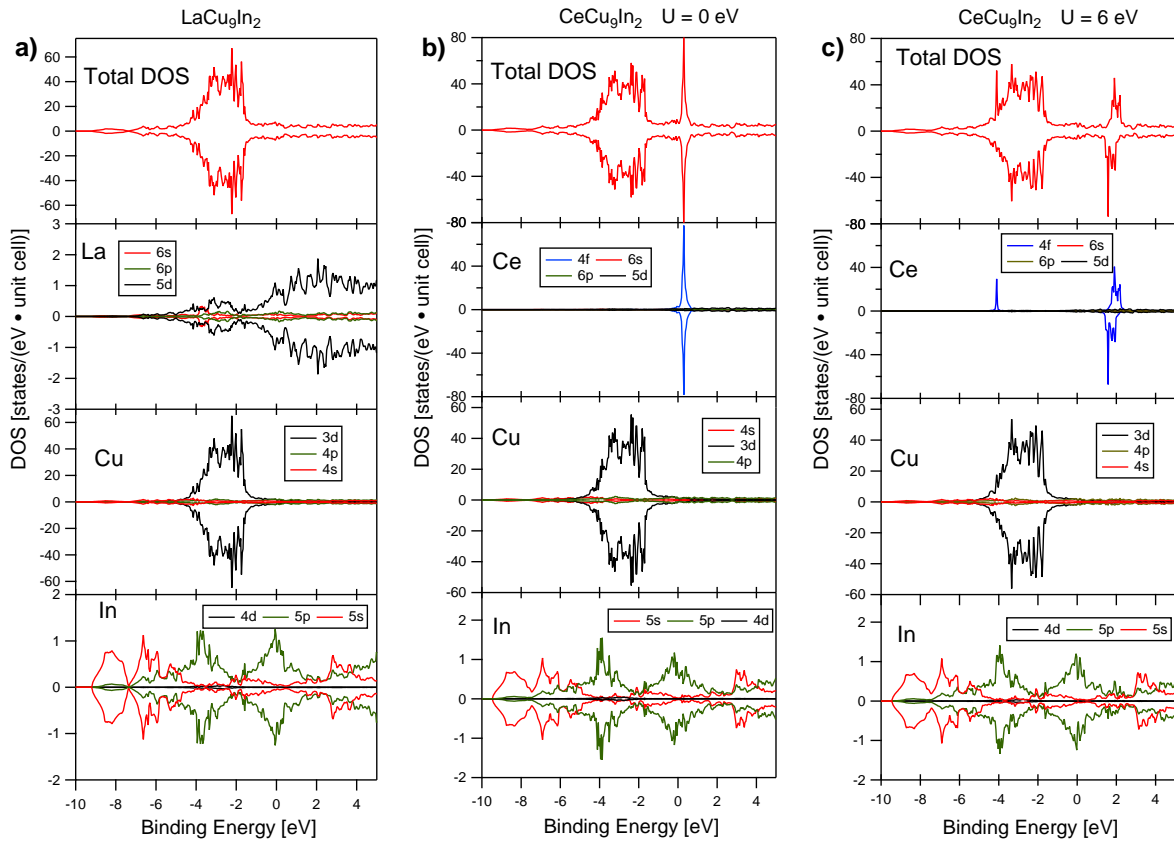


Figure 5: (Color on-line) Total and partial densities of states calculated with application of FPLO code for (a) LaCu_9In_2 and (b) CeCu_9In_2 without ($U = 0 \text{ eV}$) and (c) with ($U = 6 \text{ eV}$) additional correlations. Opposite spin directions are marked by positive and negative values of density of states.

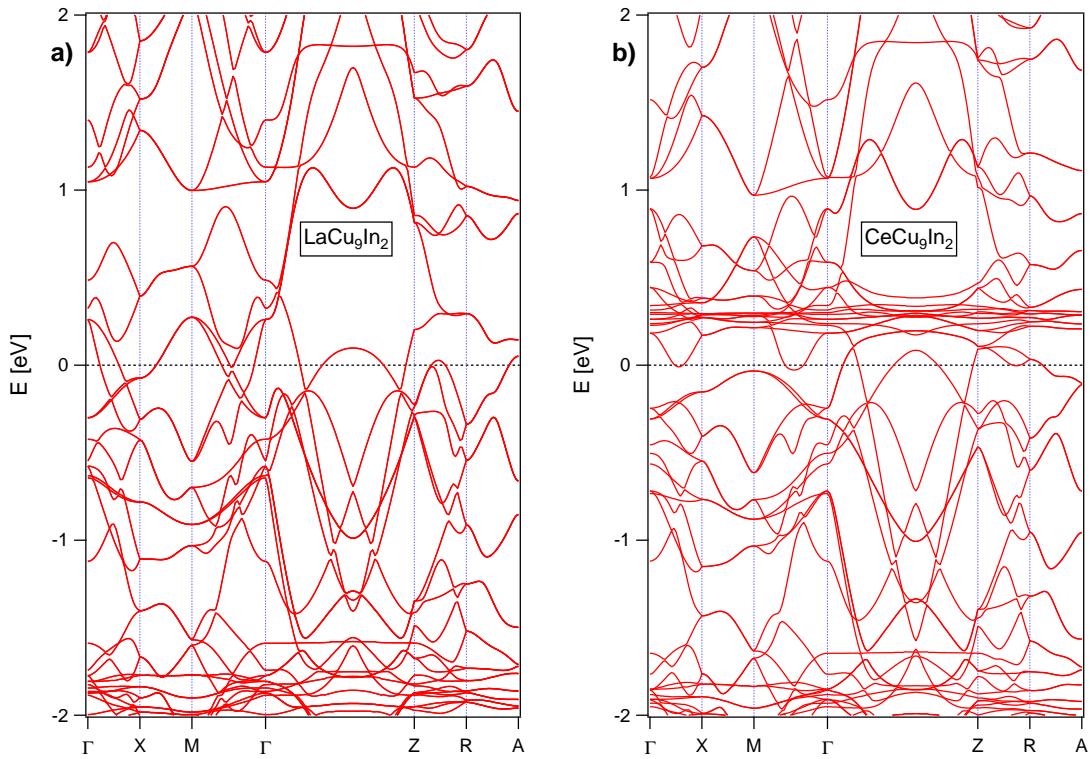


Figure 6: (Color on-line) Ground state band structures of (a) LaCu_9In_2 and (b) CeCu_9In_2 , calculated with application of Elk code. Non-magnetic ground state has been assumed.

CeCu₉In₂, there is a structure in the center of BZ, which resembles a doughnut which is flattened also in the direction perpendicular to \mathbf{c}^* . Moreover, one can see some almost flat parallel sheets of FS, which are perpendicular to \mathbf{c}^* . This fact can be interpreted as an existence of FS nesting in CeCu₉In₂.

We have computed the Sommerfeld coefficient (γ_{theor}) with application of formula derived on the basis of free electron theory using calculated total densities of states at the Fermi level ($D(E_F)$) according to the equation [40]:

$$\gamma_{theor} = \frac{k_B^2 \pi^2}{3} D(E_F) \quad (9)$$

The obtained values of the γ_{theor} coefficient are collated in the Table 2.

One can notice, that in case of LaCu₉In₂, the value of γ_{theor} is in perfect agreement with the experimental one. This means that electrons in this compound are not strongly correlated and can be properly described with application of DFT based methods. On the contrary, in case of CeCu₉In₂, there is a large discrepancy between γ_{theor} and the experimental one. Even the introduction of correlation between 4f electrons in the mean-field level does not lead to improvement of agreement between theory and experiment. It rather leads to greater discrepancy, than in case with U=0. It can be explained as follows. For U=0 eV, DOS is symmetric with respect to the spin, and one can observe some peak-like structure in Ce 4f partial DOS, which has got a maximum above the Fermi level. However, there is some non-zero density of states at the Fermi level, because of the finite width of this structure. When Coulomb repulsion on the f shell is slightly higher than 0, then this peak moves above the Fermi level (calculations for U=2 eV are not shown), which corresponds to decrease of DOS at E_F and finally to smaller value of γ_{theor} , while the actual value of γ is enhanced by the correlation effects. Moreover, increase of U leads to splitting of the peak in vicinity of the Fermi level into two peaks because lower and higher Hubbard bands are formed. The first one is located below E_F , while the second one is placed above the Fermi level. Similar situation was observed previously in case of the CeNi₉In₂ compound [9]. Discrepancy between theoretical and experimental value of Sommerfeld coefficient of CeCu₉In₂ is not startling for us and it testifies presence of strong correlations in this compound.

4. Conclusions

In order to characterize the properties of the CeCu₉In₂ system we performed experimental studies of electrical resistivity, specific heat and electronic structure. The data are complemented by DFT calculations. To separate an effect of 4f electrons similar studies have been realized for the isostructural LaCu₉In₂ reference compound. The results indicate that CeCu₉In₂ is a Kondo lattice system with the coherence temperature T_{coh} =45 K and Kondo temperature T_K \approx 5 K. Transition to the AFM state is anticipated at T = 1.6 K. Properties of a Fermi liquid are observed at low temperatures. Lattice vibrations, Kondo effect, crystal field

splitting and magnetism contribute to specific heat. Crystal field energy level scheme for CeCu₉In₂ is of the doublet-quartet type with splitting energy Δ = 50.2(1.1) K. Low temperature linear dependence of specific heat yields relatively high Sommerfeld coefficient of 132(4) mJ/(mole·K²) what points to the enhancement of the effective mass of charge carriers. Another effects of coupling between 4f electrons and conduction band are visible in the 3d core level XPS spectra and in UPS spectra of valence band. The Kondo peak, which is assigned usually to the 4f¹_{5/2} final state is not visible in raw UPS data. However, increased spectral intensity near E_F is found in the extracted spectral contribution from 4f electrons. We have observed peak at binding energy equal to -0.25 eV, which is related to the 4f¹_{7/2} final state. Theoretical calculations predict nesting of FS in case of CeCu₉In₂.

Acknowledgement

This work has been supported by the National Science Centre, Poland within the Grant no. 2016/23/N/ST3/02012. Support of the Polish Ministry of Science and Higher Education under the grant 7150/E-338/M/2018 is acknowledged. We are grateful to M. Rams for measurements of specific heat at low temperature (0.4–10 K). The research was carried out with the equipment purchased thanks to the financial support of the European Regional Development Fund in the framework of the Polish Innovation Economy Operational Program (contract no. POIG.02.01.00-12-023/08).

References

- [1] Y. M. Kalychak, V. I. Zaremba, R. Pöttgen, M. Lukachuk, R.-D. Hoffmann, Rare earthtransition metalindides, Vol. 34 of Handbook on the Physics and Chemistry of Rare Earths, Elsevier, 2004, pp. 1–133. doi:10.1016/S0168-1273(04)34001-8.
- [2] I. Bigun, M. Dzevenko, L. Havela, Ya. M. Kalychak, in: Solid Compounds of Transition Elements II, Vol. 194 of Solid State Phenomena, Trans Tech Publications, 2013, pp. 45–49. doi:10.4028/www.scientific.net/SSP.194.45.
- [3] I. Bigun, M. Dzevenko, L. Havela, Ya. M. Kalychak, Eur. J. Inorg. Chem. 16 (2014) 2631–2642. doi:10.1002/ejic.201400058.
- [4] V. M. Baranyak, Ya. M. Kalychak, Neorg. Mater. 27 (6) (1991) 1235–1238.
- [5] Ya. M. Kalychak, Izv. AN SSSR, Metally 4 (1998) 110–118.
- [6] S. Baran, J. Przewonik, Ya. M. Kalychak, Yu. Tyvanchuk, A. Szytuła, J. Magn. Magn. Mater. 410 (2016) 156–164. doi:10.1016/j.jmmm.2016.03.009.
- [7] O. Moze, S. Mentink, G. Nieuwenhuys, K. Buschow, J. Magn. Magn. Mater. 150 (3) (1995) 345–348. doi:10.1016/0304-8853(95)00297-9.

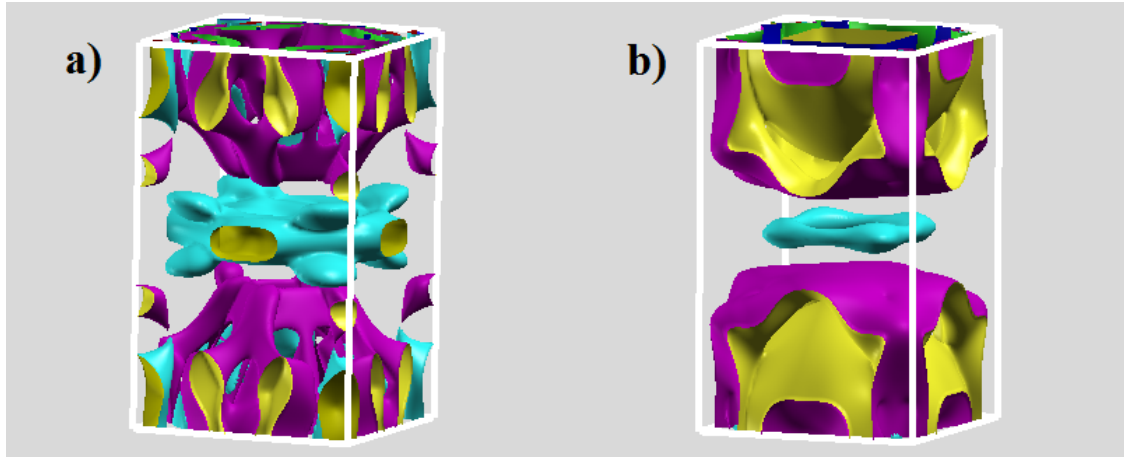


Figure 7: (Color on-line) Fermi surface of (a) LaCu_9In_2 and (b) CeCu_9In_2 , calculated with application of Elk code. Non-magnetic ground state has been assumed.

Table 2: Comparison between experimental (γ_{exp}) and theoretical (γ_{theor}) values of the Sommerfeld coefficient for LaCu_9In_2 and CeCu_9In_2 .

	U [eV]	γ_{theor} [mJ/(mole·K ²)]	γ_{exp} [mJ/(mole·K ²)]
LaCu_9In_2	0	14.08	14.0(1)
	0	19.76	
CeCu_9In_2	2	19.69	132(4)
	6	13.61	

- [8] A. Szytuła, S. Baran, B. Penc, J. Przewonik, A. Winiarski, Yu. Tyvanchuk, Ya. M. Kalychak, J. Alloy. Compd. 589 (2014) 622–627. doi:10.1016/j.jallcom.2013.12.012.
- [9] R. Kurlito, P. Starowicz, J. Goraus, S. Baran, Yu. Tyvanchuk, Ya. M. Kalychak, A. Szytuła, Solid State Commun. 206 (2015) 46–50. doi:10.1016/j.ssc.2015.01.014.
- [10] K. Koepf, H. Eschrig, Phys. Rev. B 59 (1999) 1743–1757. doi:10.1103/PhysRevB.59.1743.
- [11] V. I. Anisimov, I. V. Solovyev, M. A. Korotin, M. T. Czyżyk, G. A. Sawatzky, Phys. Rev. B 48 (1993) 16929–16934. doi:10.1103/PhysRevB.48.16929.
- [12] J. P. Perdew, Y. Wang, Phys. Rev. B 45 (1992) 13244–13249. doi:10.1103/PhysRevB.45.13244.
- [13] D. M. Ceperley, B. J. Alder, Phys. Rev. Lett. 45 (1980) 566–569. doi:10.1103/PhysRevLett.45.566.
- [14] [link].
URL <http://elk.sourceforge.net/>
- [15] N. F. Mott, H. Jones, The Theory of the Properties of Metals and Alloys, Oxford University Press, London, 1958.
- [16] G. Grimvall, The Electron-Phonon Interaction in Metals, North-Holland Pub. Co., Amsterdam, 1981.
- [17] M. Szlowska, D. Kaczorowski, Phys. Rev. B 85 (2012) 134423. doi:10.1103/PhysRevB.85.134423.
- [18] V. H. Tran, Phys. Rev. B 70 (2004) 094424. doi:10.1103/PhysRevB.70.094424.
- [19] K. Schotte, U. Schotte, Phys. Lett. A 55 (1) (1975) 38–40. doi:10.1016/0375-9601(75)90386-2.
- [20] A. P. Pikul, U. Stockert, A. Steppke, T. Cichorek, S. Hartmann, N. Caroca-Canales, N. Oeschler, M. Brando, C. Geibel, F. Steglich, Phys. Rev. Lett. 108 (2012) 066405. doi:10.1103/PhysRevLett.108.066405.
- [21] M. d. Souza, R. Paupitz, A. Seridonio, R. E. Lagos, Braz. J. Phys. 46 (2) (2016) 206–212. doi:10.1007/s13538-016-0404-9.
- [22] M. E. Huntelaar, A. S. Booi, E. H. P. Cordfunke, R. R. van der Laan, A. C. G. van Genderen, J. C. van Miltenburg, J. Chem. Thermodynamics 32 (2000) 465–482. doi:10.1006/jcht.1999.0614.
- [23] T. Toliński, A. Hoser, S. Rols, A. Kowalczyk, A. Szlaferek, Solid State Commun. 149 (47) (2009) 2240–2243. doi:10.1016/j.ssc.2009.09.002.
- [24] A. Georges, C. R. Phys. 17 (3) (2016) 430–446. doi:10.1016/j.crhy.2015.12.005.
- [25] J. J. Yeh, Atomic Calculation of Photoionization Cross-Sections and Asymmetry Parameters, Gordon and

- Breach Science Publishers, Langhorne, PE (USA), 1993.
- [26] J. J. Yeh, I. Lindau, Atomic Data and Nuclear Data Tables 32 (1) (1985) 1–155. doi:10.1016/0092-640X(85)90016-6.
 - [27] P. Starowicz, R. Kurlito, J. Goraus, H. Schwab, M. Szlawska, F. Forster, A. Szytuła, I. Vobornik, D. Kaczorowski, F. Reinert, Phys. Rev. B 89 (2014) 115122. doi:10.1103/PhysRevB.89.115122.
 - [28] G. R. Stewart, Z. Fisk, M. S. Wire, Phys. Rev. B 30 (1984) 482–484. doi:10.1103/PhysRevB.30.482.
 - [29] Y. nuki, Y. Shimizu, M. Nishihara, Y. Machii, T. Komatsubara, J. Phys. Soc. Jpn. 54 (5) (1985) 1964–1974. doi:10.1143/JPSJ.54.1964.
 - [30] F. Patthey, W. D. Schneider, Y. Baer, B. Delley, Phys. Rev. B 34 (1986) 2967–2970. doi:10.1103/PhysRevB.34.2967.
 - [31] F. Patthey, J.-M. Imer, W.-D. Schneider, H. Beck, Y. Baer, B. Delley, Phys. Rev. B 42 (1990) 8864–8881. doi:10.1103/PhysRevB.42.8864.
 - [32] E. A. Goremychkin, R. Osborn, Phys. Rev. B 47 (1993) 14580–14583. doi:10.1103/PhysRevB.47.14580.
 - [33] M. Garnier, K. Breuer, D. Purdie, M. Hengsberger, Y. Baer, B. Delley, Phys. Rev. Lett. 78 (1997) 4127–4130. doi:10.1103/PhysRevLett.78.4127.
 - [34] D. Ehm, F. Reinert, J. Kroha, O. Stockert, S. Hüfner, Acta Phys. Pol. B 34 (2003) 951–954.
 - [35] D. Ehm, S. Hüfner, F. Reinert, J. Kroha, P. Wölfle, O. Stockert, C. Geibel, H. v. Löhneysen, Phys. Rev. B 76 (2007) 045117. doi:10.1103/PhysRevB.76.045117.
 - [36] J. C. Fuggle, F. U. Hillebrecht, Z. Zohnierek, R. Lässer, C. Freiburg, O. Gunnarsson, K. Schönhammer, Phys. Rev. B 27 (1983) 7330–7341. doi:10.1103/PhysRevB.27.7330.
 - [37] O. Gunnarsson, K. Schönhammer, Phys. Rev. B 28 (1983) 4315–4341. doi:10.1103/PhysRevB.28.4315.
 - [38] S. Doniach, M. Šunjić, J. Phys. C Solid State 3 (2) (1970) 285–291. doi:10.1088/0022-3719/3/2/010.
 - [39] D. A. Shirley, Phys. Rev. B 5 (1972) 4709–4714. doi:10.1103/PhysRevB.5.4709.
 - [40] C. Kittel, Introduction to Solid State Physics, John Wiley and Sons, Inc., United States, 1996.